Polyurethane tissue adhesives for annulus fibrosus repair: Mechanical restoration and cytotoxicity

Lucas Dall Agnol[1] ![ORCID], Fernanda Trindade Gonzalez Dias[2], Natália Fontana Nicoletti[3], Daniel Marinowic[4], Sidnei Moura e Silva[1,5], Angel Marcos-Fernandez[6], Asdrubal Falavigna[1,3] and Otávio Bianchi[1,2,7,*]

Abstract
The microdiscectomy used for the treatment of intervertebral disc disorders leaves an open incision in the annulus fibrosus that must be sealed to avoid re-herniation and other subsequent degenerations. In this study, we developed an injectable and in situ polymerizable polyurethane adhesive as a long-term post-surgical annulus fibrosus repair strategy. It was investigated the chemical structure of the urethane-based adhesive and its physico-chemical, viscoelastic, kinetic, and in vitro cytotoxic properties. The adhesive formulated from the polycarbonate diol with the highest molar mass was the one that exhibited a compressive behavior closest to the intervertebral disc outer region, and therefore, the most suitable for restoration. This adhesive showed 18-day stability under moisture and required a preparation time of 10 h at 60°C before use. The material also adhered covalently to gelatin (without catalyst or initiator) and positively impacted cell proliferation after its polymerization, which are essential requirements for clinical translation. These findings confirmed the ability of the polyurethane adhesive to act as an annulus fibrosus sealant, although further improvements in its formulation are necessary.

[1]Health Sciences Graduate Program, University of Caxias do Sul (UCS), Caxias do Sul, RS, Brazil
[2]Materials Science Graduate Program (PGMAT), University of Caxias do Sul (UCS), Caxias do Sul, RS, Brazil
[3]Cell Therapy Laboratory (LATEC), University of Caxias do Sul (UCS), Caxias do Sul, Brazil
[4]Brain Institute of Rio Grande do Sul (BraIns), Pontifical Catholic University of Rio Grande do Sul, Porto Alegre, RS, Brazil
[5]Laboratory of Biotechnology of Natural and Synthetics Products, Technology Department, Institute of Biotechnology, University of Caxias do Sul, Caxias do Sul, RS, Brazil
[6]Instituto de Ciencia y Tecnología de Polímeros (CSIC), Madrid, Spain
[7]Federal University of Rio Grande do Sul, Materials engineering department, Porto Alegre, Brazil

*Lucas Dall Agnol and Otávio Bianchi contributed equally to this work.

Corresponding authors:
Lucas Dall Agnol, University of Caxias do Sul, Rua Francisco Getúlio Vargas, 1130, Postal code: 95070-560 - Caxias do Sul, BR.
Email: lucasdall1989@hotmail.com

Otávio Bianchi, University of Caxias do Sul, Rua Francisco Getúlio Vargas, 1130, Postal code: 95070-560 - Caxias do Sul, BR.
Email: otavio.bianchi@gmail.com

Introduction

Lumbar discectomy is a spinal surgery that plays a vital part in the relief of pain symptoms and motor deficit caused by intervertebral disc (IVD) herniation regardless of it is often linked to postoperative complications.[1] Re-herniation events are an unfavorable evolution of discectomy appearing in 5–15% spinal decompression surgeries that highlight the disc structure restoration is essential for annulus fibrosus (AF) and nucleus pulposus (NP) functionality.[2] These structures have specific mechanical characteristics and exhibit viscoelastic behavior to allow and control the movement of the functional vertebral bodies.[3] However, IVD itself is structurally avascular and has a precarious nutritional pathway,[4] which makes the regenerative potential of the AF and NP tissues somewhat limited. During the structural collapse of the

IVD, parts of the NP can move to defective outer parts of the AF, compressing the adjacent spinal nerves and causing inflammation. The degenerate portion of the disc can be removed through a small surgical incision (3–4 mm in diameter) in the AF, but the unrepaired defect can create changes in biomechanics and the microenvironment of IVD.[5] Therefore, sealing the compromised AF can help to restore the physiological function of the herniated IVD and prevent painful conditions for the patient.

Non-injectable AF repair approaches include sutures that do not restore intradiscal pressure[6] and plugs that have a risk of NP extrusion.[7] Injectable solutions for AF closure seem to be more promising than rigid implants since they do not require anchoring to the vertebral body, besides easily handling, nonetheless, all injectable sealants developed so far showed mechanical limitation or biological incompatibility.[8,9] Mechanical resistance and biodegradability were the two structural requirements for AF-engineered materials in most of the regeneration devices reported in the literature.[7,9] An AF repair device should be mechanically designed to provide flexibility, maintain intradiscal pressure, and withstand the daily loads experienced by the IVD.[10] The implant biodegradability, however, is a controversial requirement since it does not always meet the specificity of the application. Considering the avascular nature and slow self-repair capability of the AF microenvironment, a scaffold material with a low rate of degradation is more technically feasible.[4] Also, spine devices will remain in situ for extended periods of time, and long-term chemical stability should be guaranteed.

For an AF-engineered adhesive or sealant to be a promise of clinical delivery, it must be injectable and polymerizable under physiological conditions and present strong tissue adherence, cytocompatibility, minimal swelling, a mechanical performance comparable to the native AF, and long shelf life.[11] Initial attempts to develop tissue adhesives involved the use of cyanoacrylates, fibrin, albumin-glutaraldehyde, epoxy resins, methacrylate-based systems, but these materials were inappropriate due to their low bonding strength, degradability or high infection rates.[5] Among semisynthetic tissue adhesives, urethane-based ones have called the attention of researchers by their mechanical robustness, controlled degradation, and cell affinity. In addition, these materials provide adherence to the biological tissue through covalent bonds.[12] The wide variety of polyurethane (PU) components and processing conditions allow tailoring the adhesive formulations for the designed use. Unfortunately, only biodegradable PU sealants are thoroughly discussed in the literature.[11] PU adhesives based on the functionalization of isocyanate with oxidized dextran[13] and polyether/polyester copolymers[14–16] were developed,

but none proved to be suitable for AF repair. Contributions from specialists in biomaterials, biological, and clinical areas are necessary to create a construct which will, upon implantation, provide immediate closure of the defect and maintain the mechanical properties of the disc. Only an interdisciplinary approach can address the highly complex problem of providing an intra-operative procedure which could lead to reduced re-herniation of repaired AF tissue and decrease long-term pain for patients.[8]

This work aimed to develop a PU-based adhesive capable of mechanically sealing small AF injuries from discectomy surgical procedures. Specifically, this study comprised the production of an injectable and in situ polymerizable sealant and the validation of its performance through physicochemical (surface free energy and swelling), solid viscoelastic, mechanical, thermal, rheological, and biological (in vitro cytotoxicity) assays. These materials present interesting characteristics and will contribute to the newly emerged tissue adhesive technology. The focus of this work was to propose a sealant capable of providing mechanical stability during the AF closure, and not offering a regenerative therapy for a functional remodeled AF tissue.

Materials

The polyols Eternacoll PH50 (500 g/mol), PH100 (1000 g/mol), and PH200 (2000 g/mol), based on a mixture of 1,5-pentanediol and 1,6-hexanediol, were used as the aliphatic polycarbonate diol (PCD) and were supplied by UBE Corporation Europe (Spain); 1,6-Hexamethylene diisocyanate (HDI, 99+% purity) was purchased from Vencorex Chemicals (France). The commercial gelatin was supplied by Gelnex (Brazil). VERO (kidney epithelial cells, African green monkey) and NIH/3T3 (murine fibroblast) cell lines were purchased from The American Type Culture Collection (ATCC-Rockville, Maryland, USA). All solvents were of analytical grade, and all other chemicals were used as received.

Methods

Synthesis and structure of urethane-based materials

The urethane-based polymers were produced in the absence of organic solvents by reacting stoichiometric amounts (1.0 NCO/OH molar ratio) of HDI and PCD of different molar masses (500, 1000, and 2000 g/mol). The urethane-based prepolymers were produced by reacting PCD of 2000 g/mol with an excess of HDI (1.2–5.0 NCO/OH molar ratio). The reaction was performed by stirring PCD and HDI in a round-bottomed flask under a nitrogen atmosphere. The product was

kept in an oven at 60°C under vacuum for at least 24 h. The materials were formulated with 1.0–5.0 NCO/OH molar ratios to optimize the viscoelastic requirements for AF repair (Table 1). Only samples produced with an excess of isocyanate groups (–NCO) or prepolymers will exhibit adhesive characteristics. Fourier Transform Infrared spectroscopy in attenuated total reflectance mode (ATR-FTIR) confirmed the chemical structure of the urethane-based materials. The ATR-FTIR measurements were performed in a Perkin Elmer Impact 400 spectrometer from 4000 to 400 cm^{-1}, with 32 scans and 4 cm^{-1} resolution (diamond crystal at 45°).

The molecular weight of the polymers (U500-1, U1000-1, and U2000-1) was determined by size exclusion chromatography (SEC) in a Perkin Elmer series 200 chromatograph using dimethylformamide with 1% of BrLi as the eluent, a sample concentration of 10 mg/mL, 1 mL/min flow rate, an injected volume of 10 µL, columns temperature of 35°C, and polystyrene standards for the calibration curve.

Dynamic mechanical analysis

The viscoelastic response of the fully polymerized urethane-based samples establishes if the synthesized materials can support conditions similar to the native IVD. The dynamic mechanical properties of the solid polymers U500-1, U1000-1, and U2000-1 samples were evaluated using a DMA 242C (Netzsch, Germany) in compression mode. Specimens with cylindrical shape (15 mm diameter and 4 mm thickness) were tested. The measurements were performed at 37°C in the linear viscoelastic region, under constant strain amplitude (±30 µm) in the 0.1–10 Hz frequency range. The experiments were repeated three times for each condition. The measurements were confined to the early stages after PU-adhesive formation; long-term cycling of loads was not considered.

Polymerization reaction: Kinetics parameters and rheology

Since the adhesive is intended to be applied in therapy, it becomes essential to know its: (i) preparation time and (ii) final viscosity when the entire limiting reagent (–OH groups from PCD) is consumed after polymerization. The adhesive preparation time was simulated by monitoring the polymerization kinetics of samples U500-1, U1000-1, and U2000-1 using differential scanning calorimetry (DSC). The DSC experiments were performed with ~10 mg of sample in a DSC-50 Shimadzu instrument under nitrogen atmosphere (50 mL/min). The materials were sealed in aluminum crucibles and heated from 25 to 180°C under nonisothermal conditions, using four different heating rates (5, 10, 15, and 20°C/min). The kinetic parameters of the reactions were computed using "Netzsch Thermokinetics: A Software Modulus for the Kinetic Analysis of Thermal Measurements". The activation energy ($E_{\alpha(T)}$) values were determined through integral and differential model-free isoconversional methods. The Flynn–Wall–Ozawa (FWO),[17] Friedman (FR),[18] and Kissinger–Akahira–Sunose (KAS)[19] methods were used to establish the $E_{\alpha(T)}$ dependence with the conversion degree, $\alpha_{(T)}$. The corresponding kinetic parameters were evaluated by a "Multivariate Nonlinear Regression" program, which uses a hybrid Marquardt–Levenberg approach. The best kinetic model was chosen by the least squares and F-test method. The kinetics model equations employed by the software are shown in supplementary files (Table S1).

The rheological profiles of the U2000-1 and U2000-2 materials were investigated in an Anton Paar MCR301 rheometer coupled with plate-plate geometry (diameter 25 mm, gap 1 mm). The isothermal experiments were performed within the linear viscoelastic regime (small stress 50 Pa) under dynamic oscillation mode using a 1.0 Hz frequency at 37.5 and 60°C.

PU–collagen adhesion strength

The adhesion strength tests determine how strongly the sealant adheres to collagen tissue and can be characterized by its resistance to traction when glued between two gelatin sheets.[20] The adhesiveness of urethane-based prepolymers was evaluated by tensile strength tests using a Universal Testing Machine Emic

Table 1. Description of the formulated polyurethane samples.

Samples	NCO/OH molar ratio	PCD molar mass (g/mol)	Consistency of the materials
U500-1	1	500	Solid
U1000-1	1	1000	Solid
U2000-1	1	2000	Solid
U2000-1.2	1.2	2000	Adhesive gel
U2000-2	2	2000	Adhesive gel
U2000-3	3	2000	Adhesive gel
U2000-5	5	2000	Adhesive gel

DL2000. The U2000-1.2, U2000-2, U2000-3, and U2000-5 samples were applied to the tip of gelatin sheets (7 cm × 2 cm) using a spatula, covering an area of approximately 4 cm². The gelatin sheets were prepared by a solution casting method (10 g of gelatin dissolved in 100 mL of distilled water) at room temperature. The tips of the bonded sheets were then pressed together at 37.5°C for 36 h to allow attachment and polymerization of the adhesive to the substrate. The system was subjected to traction using a 12 mm of grip-to-grip separation and a 20 mm/min crosshead speed. Gelatin-adhesive interfacial failure was quantified via uniaxial tensile tests on gelatin-adhesive-gelatin constructs. The possible reactions and intermolecular interactions between gelatin and urethane-based prepolymers were investigated by ATR-FTIR. The surface of the gelatin sheets in contact with the adhesive was immersed in dimethyl sulfoxide (DMSO) solvent to remove the urethane phase. The solvent treatment only extracted the non-bonded PU materials. Thus, the functional groups (urea and amide) formed by the reaction between the PU and collagen were identified by means of ATR-FTIR.

Physicochemical properties

The surface free energy of the urethane-based adhesives and gelatin sheets was determined by the Owens–Wendt method, which is based on contact angle measurements conducted with certain standard liquids.[21] The wettability behavior of the solid specimens provides a better understanding of adhesion phenomenon and biocompatibility. The contact angle measurements were carried out in an SEO® Phoenix100 (Korea) instrument, and four probe liquids were employed at $23 \pm 2°C$: distilled water ($\gamma_L{}^P = 51.0$ mJ/m², $\gamma_L{}^D = 21.8$ mJ/m², and $\gamma_L = 72.8$ mJ/m²), glycerin ($\gamma_L{}^P = 29.7$ mJ/m², $\gamma_L{}^D = 33.6$ mJ/m², and $\gamma_L = 63.3$ mJ/m²), DMSO ($\gamma_L{}^P = 8.0$ mJ/m², $\gamma_L{}^D = 36.0$ mJ/m², and $\gamma_L = 44.0$ mJ/m²), and hexadecane ($\gamma_L{}^P = 0.0$ mJ/m², $\gamma_L{}^D = 27.6$ mJ/m², and $\gamma_L = 27.6$ mJ/m²); where $\gamma_L{}^P$, $\gamma_L{}^D$ and γ_L represent the polar component, the dispersive component, and the surface free energy of the liquids, respectively.[22] The sessile drop method was adopted using 2 μL drops. The contact angle was measured at least 10 times at different sites on the surface for the consideration of the average value.

Information about the swelling behavior of the adhesive is needed to prevent any damage to the surrounding tissues due to a volume variation. The U2000-1 sample was primarily dried until constant weight at 60°C under vacuum conditions (W_s being the weight of the dry sample) to assess its water sorption capacity. The dried sample was then placed in a container with a saturated solution of pentahydrated copper sulfate and weighted at different times (W_d) until reaching a maximum weight. The water uptake (WU) was calculated using equation (1)[23]

$$WU = \left(\frac{W_s - W_d}{W_d} \right) \times 100\% \qquad (1)$$

Since the adhesives containing isocyanate end groups present the ability to react with air moisture, it is crucial to determine how their reactivity will influence the manipulation or storage events. The stability of the –NCO groups was evaluated by maintaining the U2000-2 sample in a sealed container under a water saturated atmosphere. The ATR-FTIR band at 2260 cm^{-1} was monitored at different intervals until the –NCO groups were no longer detected, attesting the end of the reactivity of the material.

General cell culture protocols

VERO (kidney epithelial cells, African green monkey) and NIH/3T3 (murine fibroblast) cell lines were purchased from American Type Culture Collection (ATCC-Rockville, Maryland, USA). The cells were cultured in Dulbecco's Modified Eagle Medium with 10% fetal bovine serum, 100 U/mL penicillin and 100 μg/mL streptomycin, at a temperature of 37°C, a minimum relative humidity of 95%, and an atmosphere of 5% CO_2 in air. PU biomaterials were disinfected with 70° ethanol and exposed to UV light for 30 min each side, in a class II safety cabinet. The cell lines were seeded at $3–5 \times 10^3$ cells per well in 96-well plates, or $15–20 \times 10^3$ cells per well in 24-well plates, depending on the experimental protocol. All experiments were performed in triplicate and repeated three times.

In vitro cytotoxicity

For adhesives to be used in vivo, its presence should not elicit any deleterious effect on cells functions. To assess cell viability, the VERO and NIH/3T3 cell lines were evaluated by their metabolically active mitochondria using an MTT assay. The cell lines were incubated with U2000-1 and U2000-2 samples by elution methods (3 cm²/mL), as recommended by ISO 10993 (2009). The results are expressed as the percentage of cell viability in relation to the positive control. The experiments were analyzed by one-way analysis of variance (ANOVA) followed by Bonferroni's post-hoc test, using Graph-Pad Software (San Diego, USA). Results are reported as the mean ± standard deviation (scanning electron microscopy (SEM)). $P < 0.05$ was indicative of statistical significance.

Nuclear morphology and mitotic index

The 40,6-diamino-2-phenylindole (DAPI) staining was carried out to establish the mitotic index as a parameter of cell proliferation. Briefly, VERO and NIH/3T3 were seeded in 24- and 96 well plates and incubated with the polymer materials for 24 h. After incubation, the cells were washed three times in PBS, and fixed with 4% formaldehyde at room temperature, for 15 min. The fixed cells were then washed with PBS, permeabilized with 0.1% Triton X-100 in PBS and stained with a 300 nM DAPI solution (Santa Cruz, CA, USA) at room temperature, for 10 min. The nuclear morphology of the cells was examined under a fluorescent microscope (Carl Zeiss MicroImaging GmbH, Germany). DAPI staining delineates mitotic figures and enables mitotic index determination for each automatic cell count. The mitotic index was calculated as the number of mitotic events in 10 fields per well, three times in triplicate. The experiments were analyzed by ANOVA followed by Bonferroni's post-hoc test, using Graph-Pad Software (San Diego, USA). The results were reported as the mean ± standard deviation (SEM). $P < 0.05$ was indicative of statistical significance.

Polymer-cell morphology

To verify polymer-cell morphology, the materials were held in a deep 24-well plate, and the NIH/3T3 cells were seeded on the U2000-2 materials at a density of $15–20 \times 10^3$ cells per well, and cultured for 24, 48, and 72 h. The topology of the systems was assessed by field emission gun scanning electron microscopy (FEG-SEM; Mira 3 Tescan, Czech Republic) and DAPI staining under fluorescence microscopy (Carl Zeiss MicroImaging GmbH, Germany). Before FEG-SEM evaluation, the materials were fixed with 2.5% glutaraldehyde, sequentially dehydrated in increasing concentrations of ethanol (50, 70, 85, 95, and 100%), and then coated with gold using a plasma sputtering apparatus. To evaluate cell presence by DAPI staining, the cells were fixed with 4% formaldehyde and stained with a 300 nM DAPI solution (Santa Cruz, CA, USA) at room temperature for 10 min.

Results and discussion

### Urethane-based materials production and characterization

The polymers (U500-1, U1000-1, and U2000-1) and prepolymers (U2000-1.2, U2000-2, U2000-3, and U2000-5) were produced from PCD and HDI monomers using an stoichiometric amount in the case of the polymers, or an excess of –NCO groups ($1 \leq$ NCO/OH ≤ 5) in the case of prepolymers to ensure that part of them was free to react with biological tissue (see Scheme S1 in supplementary files). The prepolymer structure was qualitatively examined by ATR-FTIR technique (see Fig. S2 in supplementary file). The formation of the adhesive was confirmed by the decrease in intensity of the isocyanate ($2261 \, \text{cm}^{-1}$) and the disappearance of the hydroxyl ($3489 \, \text{cm}^{-1}$) bands. When the adhesive loses its reactivity, which can be attested by the disappearance of the $2260 \, \text{cm}^{-1}$ band, new peaks appear around $3328 \, \text{cm}^{-1}$ (N–H stretching), $1242 \, \text{cm}^{-1}$, and $1581 \, \text{cm}^{-1}$ referring to the urethane group. The band at $1242 \, \text{cm}^{-1}$ (C–O stretching from carbonate group) is also found on the PCD spectrum.[24,25]

The molecular weights (M_w) of samples U500-1, U1000-1, and U2000-1 determined by SEC were 15,2150, 17,8251, and 16,5022 g/mol, respectively. The polydispersity index (M_w/M_n) of all samples was ~ 1.59. No gel formation was observed for the samples. Thus, regardless of the molecular weight of the polyols, the PUs reached high molecular weight when stoichiometric amounts of hydroxyl and isocyanate groups are used, demonstrating that the polymerization occurred efficiently and was completed in the reaction conditions.

PU-based adhesive as an annulus fibrosus sealant

Dynamic mechanical response. The mechanical performance of the materials was evaluated through the compressive modulus, by simulating slightly higher efforts than typical physiological loading. Figure 1 shows the storage modulus of the PU polymers synthesized from different polyols as a function of frequency. Frequencies at $1 - 10$ Hz are usually observed in common daily activities.[26] All samples showed a linear increase of storage
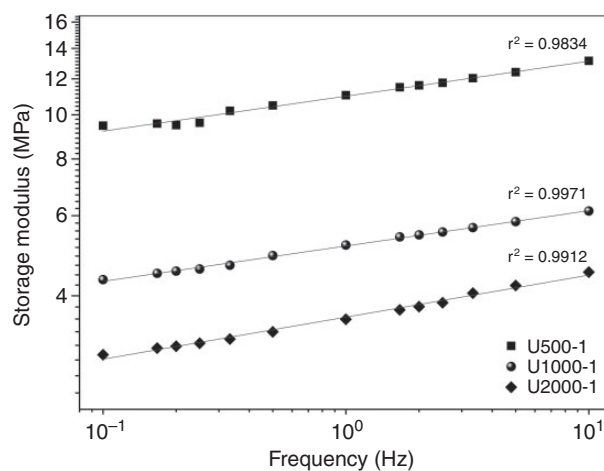
Figure 1. Storage modulus for U500-1, U1000-1, and U2000-1 solid samples.

modulus with frequency and also a pseudo-solid like behavior in these experimental conditions. This behavior concerning storage curves has already been reported for an ex vivo sheep model at 0.1–10 Hz frequency range.[27]

The average compressive modulus for the samples U500-1, U1000-1, and U2000-1 was 12.4 ± 3.6 MPa, 5.0 ± 2.4 MPa, and 3.1 ± 2.3 MPa, respectively. Clearly, the compressive modulus increases with the increase in urethane groups (or decrease in PCD length) in the polymer. These values are superior to similar tests performed on native IVD tissue.[26] The compressive modulus of U2000-1 sample was the closest to the IVD outer region $(0.22 - 0.54$ MPa$)$[28] and thus, the most adequate for restoration. PU-based materials have the versatility of being compositionally tuned to acquire mechanical properties close to those of native AF. From now on, only sample U2000-1 will be characterized, since it proved to be the most adequate in terms of mechanical properties.

Reactivity with collagen tissue. An AF repair sealant must firmly adhere to the native tissue to resist stresses generated from IVD intradiscal pressures during physiological loading. This adhesiveness is an essential requirement for clinical translation. The tensile strength results were not dependent on the NCO/OH molar ratio of the prepolymer and consequently on the amount of free –NCO groups. As a result, no clear difference could be discerned between the formulations tested. A tensile strength magnitude of 21.31 ± 3.06 MPa was reached in the rupture of gelatin sheets by fracture, not by detachment. This indicated that the adhesive strength of PU-based materials to gelatin was stronger than their cohesive strength (strength of adhesive–adhesive bonds). Here, gelatin was used to simulate the living tissue.[20,29] In all tests, the glued area in the specimens remained intact, which indicates the excellent adhesive capacity of the materials. A cohesive failure then prevailed in the mechanical test and the gelatin sheets fractured, but PU-based adhesive was still present on the surfaces of the detached pieces. For a sealant to be effective in restoring the AF, it must have a tensile strength of about 4.0–8.0 MPa and an adhesion force of 177 kPa.[30,31]

Free –NCO contents higher than NCO/OH $= 1.2$ did not contribute to adhesiveness because gelatin itself has limited reactivity. Gelatin contains approximately $31 - 35$ free amine groups and $77 - 118$ carboxylic acids per 1000 amino acids depending on the pre-treatment received during its production.[32,33] Besides increasing toxicity, high concentrations of free –NCO groups also significantly affect the viscoelastic behavior of the material. Low concentrations of free –NCO produce high viscosity prepolymers, which make the gel penetration difficult in the incision

to be sealed. Prepolymers produced with high –NCO contents, however, have low viscosity and flow through AF adjacent tissues. The U2000-2 proved to be the most appropriate sample when the parameters injectability and adhesiveness were considered.

To advance tissue adhesive technology, understanding the physicochemical interactions at the collagen/biomaterial interface is indispensable. From ATR-FTIR spectroscopic evaluation, the probable bonding mechanism between the polymer and collagen functional groups can be monitored.[34] It is assumed that the free isocyanate groups of the adhesive will react with the –NH$_2$, –OH, –COOH or –NHCO– groups present in sulfated glucosaminoglycans IVD tissue, yielding urethanes, ureas, and amides groups, as well as biuret and allophanates secondary products.[20,35] Figure 2 shows the spectra of gelatin, U2000-2 adhesive, and the gelatins surface in which the glued PU was solvent extracted. The spectroscopic results corroborated previous evaluations of the collagen/PU bonding chemistry.[32,36,37] Figure 2 attests the reaction of the carboxylic group of collagen by the narrowing of the broad $3700 - 2500$ cm^{-1} region (related to the carboxylic group asymmetric stretching) in the spectrum of the extracted gelatin sheet.[38] The gelatin sheets were previously dried to remove any traces of moisture. Bands at 3326, 1620, 1570, 1242, $732 - 790$, and 620 cm^{-1} corresponding to urea and amide groups, namely N–H stretching vibration, amide I, amide II, amide III, amide IV, and amide V, respectively, were detected.[32] The C=O groups of the urethane bonds appear at about 1730 cm^{-1} and 1740 cm^{-1} in the adhesive and extracted gelatin sheet spectra, respectively.[39] Since there is no peak at 2260 cm^{-1}, it may be said that all free –NCO groups from the adhesive have reacted.[40] Therefore, these results prove the presence of urea and amide functional groups on the gelatin/adhesive glued
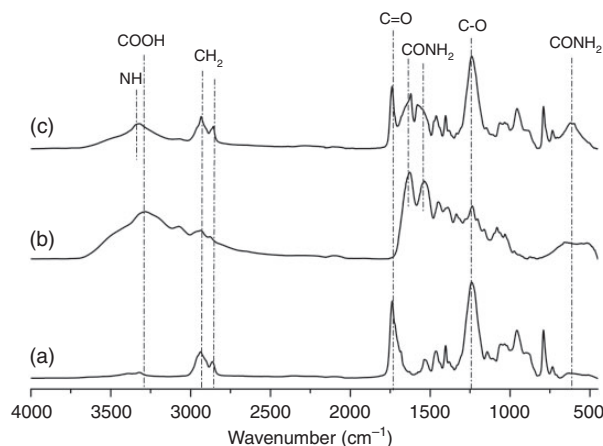
Figure 2. ATR-FTIR spectra of: (a) U2000-2, (b) gelatin, and (c) extracted gelatin sheet.

interface.[37] Only a strong covalent bond between gelatin and adhesive could explain the sheets breakage rather than its detachment when subjected to traction.

Behavior when in contact with water. Figuring out how a biomaterial behaves in an aqueous environment is essential to predict its stability under physiological conditions. The affinity of biological molecules for an implanted scaffold is profoundly affected by the nature of the biomaterial surface. Increased adhesive wettability also improves implant tissue integration. The Owens–Wendt theory determines the polar and dispersive contributions to the surface free energy of a solid using the known polar and dispersive components of the probe liquids and their contact angles with the solid.[21] The higher the surface free energy value, the higher the adhesiveness and bioactivity of a biomaterial.[20] The adhesive and the collagen sheet presented total free surface energies of 61.8 and 46.2 mN/m, respectively (Table 2), which is in agreement with the literature values.[20,24] The surface tension of blood assessed in a group of 150 healthy people (72 men and 78 women aged from 20 to 65 years) by the drop-weight method at a temperature of 22°C was 63.8 mN/m.[41] As these substrates present a very close surface energy values, it can be inferred that the adhesive will present an acceptable spreadability when in contact with the biological tissue. The polar component of the PU-based adhesive is significantly higher than its dispersive element, which explains the weak cohesion forces in this polymer, and why the adhesion forces are preferred.[20]

An excessive volume increase of the material when in contact with the physiological environment may damage the surrounding tissues. Structural changes of the adhesive can also compromise its mechanical properties. The adhesive presented a low swelling ratio of approximately $1.03 \pm 0.06\%$, which suggests that there will not be a significant volume increase capable of preventing its use. However, the adhesive will continue to present some hydrophilicity, which ensures its biocompatibility through interactions between the hydrated network and tissue proteins.[20]

Analyzing the stability of –NCO groups under humidity conditions is of paramount importance when considering the ability of urethanes to favor the adhesion with living tissues. When exposed to a saturated water atmosphere, the free isocyanate end groups of the pre-polymer react with moisture, leading to the formation of an unstable carbamic acid that decomposes to carbon dioxide and an amine group.[35] Further reactions with additional –NCO groups result in urea groups and their secondary reaction products.[42] Although this moisture reaction phenomenon will necessarily occur in the living tissues, it is essential to avoid it while the adhesive is only being manipulated or stored. The stability of the –NCO groups was monitored by ATR-FTIR technique, through the evolution of the peak at $2260 \, cm^{-1}$ relative to the free isocyanate. After 24 h under moisture atmosphere, almost 10 mol% of the –NCO groups reacted. On the seventh day, this percentage increased to 51 mol%. The conversion rate of the –NCO group decelerates over time. Initially, few monomers are polymerized, and the viscosity of the reactional medium is rather low, which allows reactants to flow and mix quickly. As the polymerization progresses, the medium becomes more viscous, and the reaction rate decreases. The total reaction of the isocyanate groups with water occurred after 18 days. When in contact with the living tissues, however, it is expected that in situ polymerization of the adhesive occurs much faster since the isocyanate reactivity with amines ($-NH_2$) is 1000 times faster than its reactivity with water and a primary hydroxyl group. Moreover, the reaction between –NCO and amino groups is thermodynamically favorable at ambient temperature and does not need to be catalyzed.[38]

Preparation conditions for clinical use. Here we discuss two parameters involved in the preparation of adhesives: (a) time between intended use and application, which was simulated by mathematical modeling of the DSC measurements and (b) viscosity, which is directly related to the injectability of the prepolymer. Concerning the time of preparation, it is essential to consider the type of clinical procedure to which the adhesive's application is linked. Microdiscectomy, because it is an elective procedure, allows for planned and previous preparation of the adhesive. The polymerization kinetic mechanism indicated in the DSC results determined the

Table 2. Contact angles (θ, °C) and surface free energy (γ_S) of the solid surfaces, including dispersive (γ_S^D) and polar (γ_S^P) contributions.

| Solid surfaces	Contact angle (θ, °C)				Surface free energy (mN/m)			
	Water	Glycerin	Dimethyl sulfoxide	Hexadecane	γ_S	γ_S^D	γ_S^P	R^2
U2000-1	74.8 ± 0.8	88.6 ± 0.8	44.6 ± 0.8	13.9 ± 0.8	61.8	10.5	51.3	0.9872
Collagen sheet	87.1 ± 0.8	80.7 ± 0.8	51.3 ± 0.8	17.2 ± 0.8	46.2	6.4	39.9	0.9935
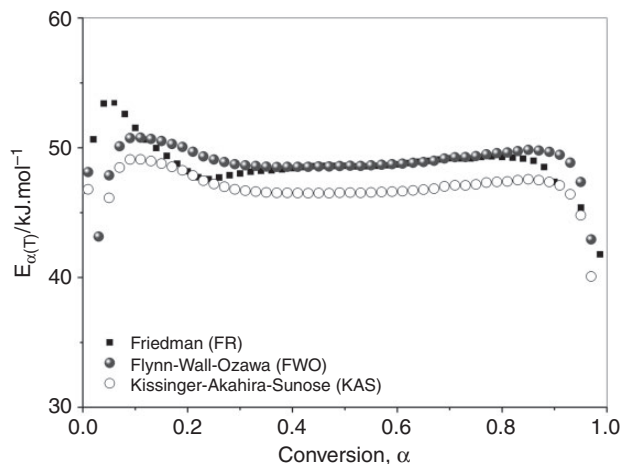
**Figure 3.** Dependence of the $E_{\alpha(T)}$ vs. $\alpha_{(T)}$ for U2000-1 sample.

Table 3. Nonisothermal kinetic parameters obtained from nonlinear regression method.

$f(\alpha)$	$E_{\alpha(T)}$ (kJ mol^{-1})	log A (s^{-1})	Correlation coefficient (r)	F test
B_{na} (n = 1.2042, a = 0.3485)	49.39	4.20	0.9867	1.00
C_{nB} (n = 1.5372, log K_{cat} = 0.6678)	50.21	3.78	0.9830	1.35
F_n (n = 1.0715)	64.89	5.97	0.9759	2.24
F_2	90.11	9.33	0.9442	3.60
A_n (n = 1.2915)	48.39	3.84	0.9805	1.49
F_1	62.60	5.67	0.9762	2.19
C_{1B} (log K_{cat} = 6.83E-3)	51.70	4.14	0.9768	2.05
D_3	132.76	13.43	0.8202	10.76
D_{3F}	131.04	13.05	0.8053	11.23
D_{1F}	112.47	10.88	0.7982	12.79
R_3	51.80	3.74	0.9596	3.44
A_2	33.50	1.90	0.8853	4.72
R_2	46.80	3.24	0.9316	4.95
D_4	124.27	12.29	0.7675	14.13
D_2	98.74	9.73	0.5243	26.55
A_3	23.89	0.65	0.6470	13.53
D_1	103.85	10.45	0.5591	25.76
B_1	−1.40	0.00	−0.5799	37.44

adhesive preparation time. Figure 3 shows the dependence of the $E_{\alpha(T)}$ vs. $\alpha_{(T)}$ for U2000-1 material. $E_{\alpha(T)}$ values were determined using the FWO, FR, and KAS isoconversional model-free methods and presented a practically constant value of $\sim$49 kJ mol^{-1}. These results are in agreement with the literature for polymerizations reactions of PU-based prepolymers.[43] The constant behavior of $E_{\alpha(T)}$ vs. $\alpha_{(T)}$ curves suggests that polymerization is limited by a single step process.[44] Also, the $E_{\alpha(T)}$ values provided by the FWO, FR, and KAS methods were quite close, proving the accuracy of
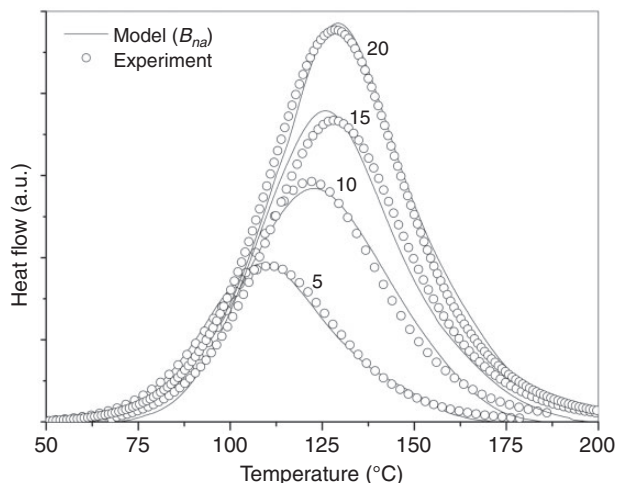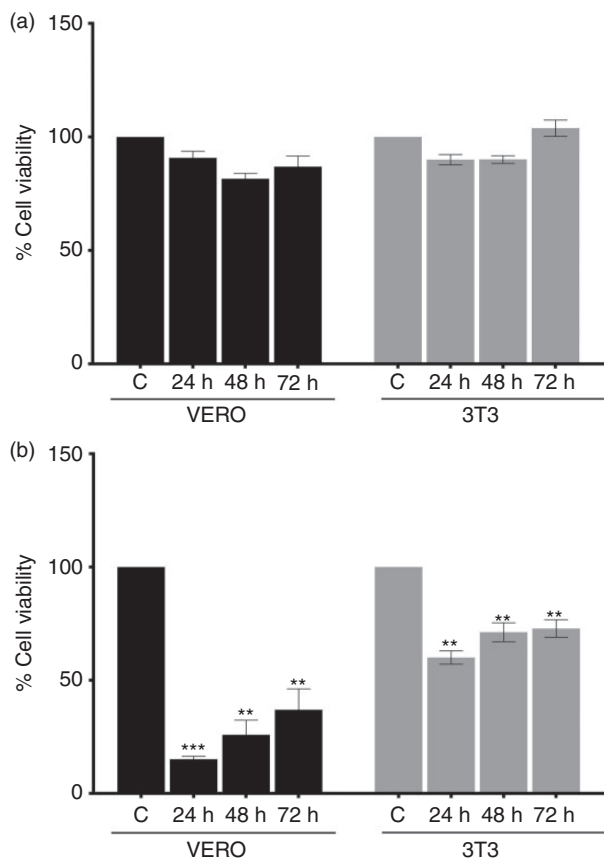

Figure 4. Model prediction of U2000-1 polymerization reaction using Prout–Tompkins (B_{na}) *n-th* order approach. The different heating rates (in °C/min) employed at DSC experiments were indicated in each curve.
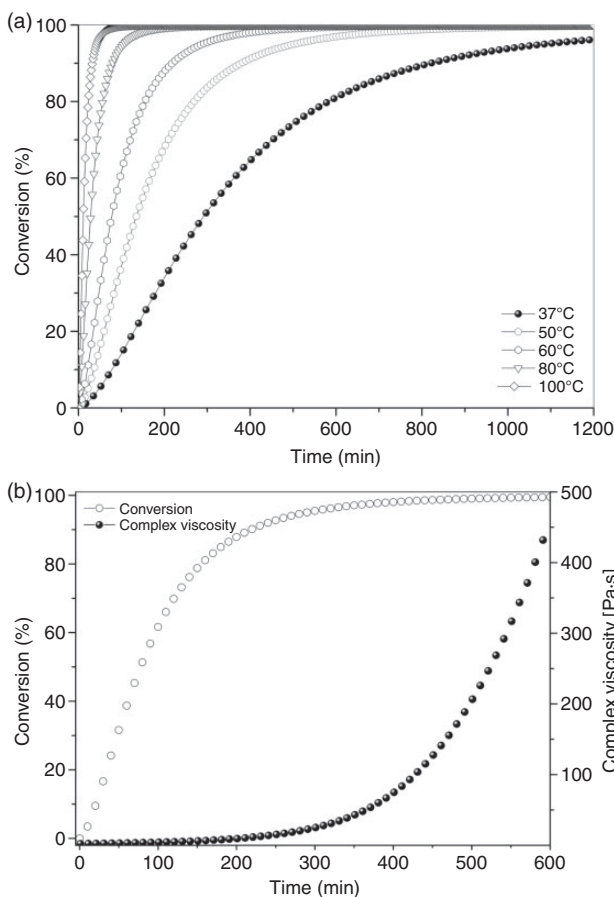
Figure 5. (a) U2000-1 reaction simulation at different temperatures and (b) U2000-1 rheological profile as a function of conversion at 60°C.

Figure 6. Effect of incubation with (a) U2000-1 and (b) U2000-2 on cell viability of NIH/3T3 fibroblast and VERO cells after 24, 48, and 72 h. Each column represents the mean ± SEM. *p < 0.05 vs. control (C).

the models. The $E_{\alpha(T)}$ values found for the U500-1 and U1000-1 remained between 55 and 60 kJ mol^{-1}.

Then, the nonisothermal kinetic parameters were investigated through multivariate non-linear regression (see Table S1) using the DSC data obtained at different heating rates. The accuracy of the 18 kinetics models adopted for determining the kinetic parameters was validated using F statistical test. Considering the correlation coefficient (r) and F-test values given in Table 3, it could be concluded that the model proposed by Prout–Tompkins (B_{na} mechanism) was the most appropriate for describing the polymerization mechanism. This model presented r and F-test values close to 1, and an activation energy ($E_{\alpha(T)}$) values nearest to those found in the FWO, FR, and KAS models.

Figure 4 shows a comparison between results obtained experimentally by DSC and those simulated mathematically by the B_{na} model. An almost perfect overlapping between experimental and theoretical data was observed, suggesting that B_{na} model can satisfactorily describe the polymerization kinetics of the

adhesive. It is not surprising that this model has been the most appropriate since it is known in the literature for describing autocatalyzed (sigmoidal shape) reactions.[43] The polymerization of urethane materials is based on an equilibrium reaction of isocyanate and alcohol chemical groups that has an autocatalytic behavior.[43]

The non-isothermal results obtained from B_{na} model were then used in simulations to predict an isothermal polymerization behavior. Figure 5(a) shows the effect of temperature on the reactional conversion and, consequently, on the preparation time of the adhesives. It can be observed that U2000-1 sample needs ~600 min at 60°C to reach a full conversion. In this condition, the material displays a viscosity of 461.3 Pa·s (liquid like behavior, Figure 5(b)) and can be injected using a needle-free syringe of 12.34 mm inner diameter. Sample U2000-2 was expected to be less viscous than sample U2000-1, which was not observed. This sample may have reacted with the humidity in the rheometer, decreasing the number of free –NCO groups on the adhesive.[35] At 37°C, the U2000-1 material polymerizes slowly, and a 461.3 Pa·s viscosity is only achieved within 1097 min of the reaction (results not shown).

In vitro cytocompatibility. The cytotoxic effects of the adhesives were evaluated by MTT assay using NIH/3T3 and VERO cell lines. The U2000-1 (non-reactive sample) and U2000-2 (adhesive, reactive sample) materials were tested, and the influence of free –NCO groups on cell response evaluated. The solid U2000-1 did not display any cytotoxicity in fibroblast NIH/3T3 and VERO lineages in up to 72 h, as shown in Figure 6 (a). When the sample containing reactive isocyanate end groups was added to the medium, significant cytotoxicity was observed for VERO cells, being this effect less pronounced for NIH/3T3 cells (Figure 6(b)). Interestingly, this cytotoxic response coincides with the time required by the prepolymer to react, as showed in the kinetic analysis. During polymerization, the pH of the biological environment drops due to the formation of carbamic acid, negatively impacting cell viability.[36,45] The CO_2 generated during the in situ reaction might also harm cell survivability. Guo et al.[46] cytoprotected cells during polymerization by encapsulating them in alginate beads to provide a barrier to CO_2 diffusion. Cells survived the polymerization at >70% viability, and rapid dissolution of alginate beads after the scaffold cured created interconnected macropores that facilitated cell adhesion to the biomaterial in vitro. Moreover, any residual monomer released from the underpolymerized material is incorporated into the lipid bilayer of the cell membrane, causing its solubilization and death.[45,47] Nevertheless, enhancement of cell viability after 48 h
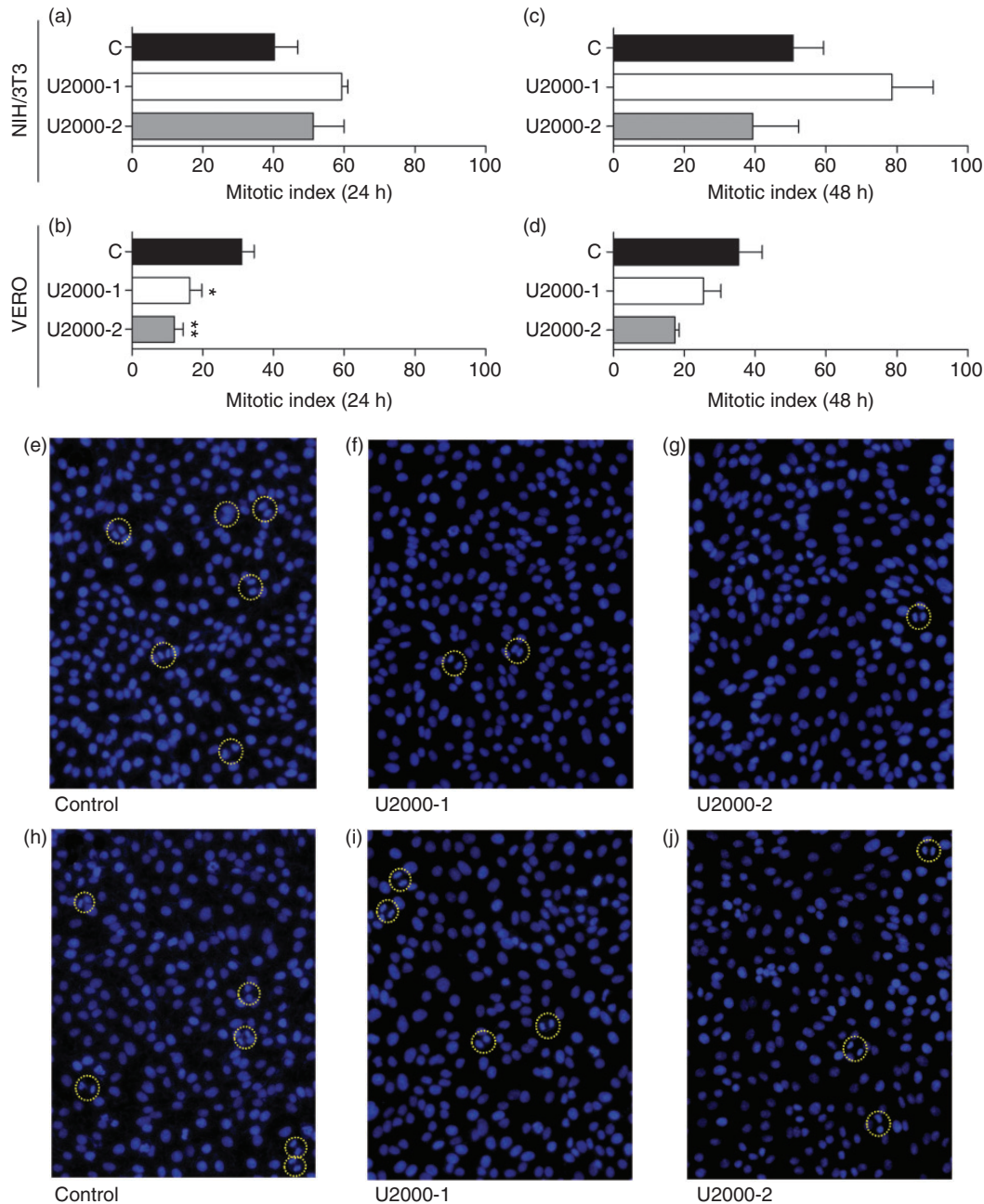
Figure 7. Frequency of mitotic cells as a parameter of cell proliferation after (a,b) 24 h and (c,d) 48 h of incubation with U2000-1 and U2000-2. The mitotic index was established for NIH/3T3 and VERO cell lines. Each column represents the mean ± SEM. *p < 0.05 vs. control (C). Representative images of VERO cells showing mitotic figures (yellow circles marking) in late anaphase with the appearance of two discs migrating toward opposite poles of the cell on 24 h of (e) control, (f) U2000-1, (g) U2000-2 and 48 h of (h) control, (i) U2000-1, (j) U2000-2 (magnification 20×).

was denoted for both VERO and NIH/3T3 lineages, a phenomenon already reported earlier in the literature.[40,48]

To reinforce the biological compatibility, a proliferative cell profile by the mitotic index was determined. Both non-reactive (U2000-1) and reactive (U2000-2) biomaterials markedly reduced the mitotic index in VERO cells in the first 24 h after exposure, confirming that polymerization interacts negatively in a cell cycle-dependent manner for this cell type. However, the morphological profile of this cells might indicate just a downregulation on cell-cycle progression (stoped between G0/G1) as a protective mechanism, since quickly after 48 h post-exposure the frequency of

mitotic cells seems to be initially restored (Figure 7). It is known that reversible protein phosphorylation events play a crucial role in intracellular check-point signal pathways that regulate cell-cycle progression and, consequently, the proliferative potential. Of note, the NIH/3T3 cells exposed to U2000-1 and U2000-2 showed a frequency of mitotic events similar to the negative control group (Figure 7), confirming that the cellular response is metabolism dependent. Representative images of mitotic events are shown in Figure 7, considering only late anaphase events, with the appearance of two discs migrating toward opposite poles of the cell.
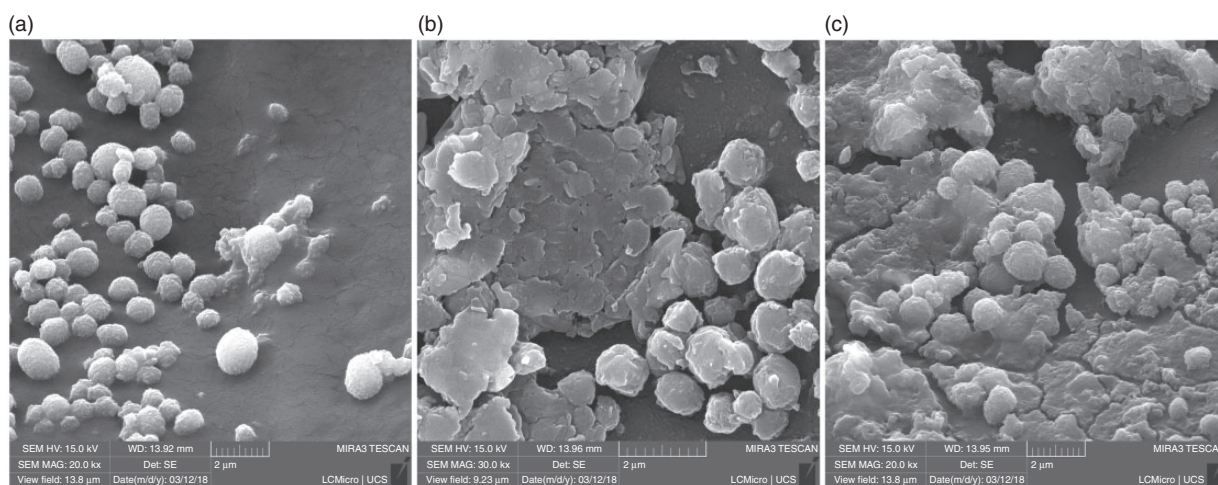
DAPI staining is also a tool that provides nuclear morphological features (area, eccentricity, and solidity) and might be related to several mechanisms that affect cell survival processes. The VERO cells exposed to
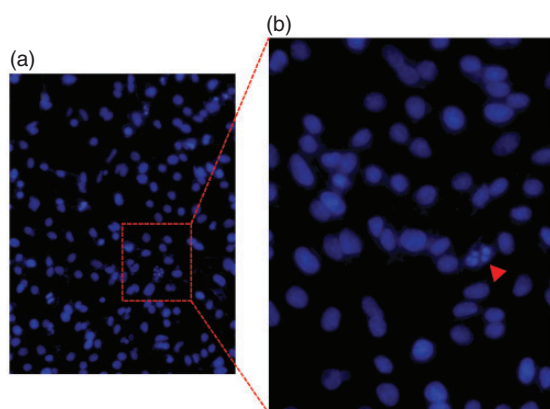
reactive U2000-2 for 24 h presented raised morphological signs of apoptosis with disintegrated nuclei which is due to the presence of cytoplasmic blebs (bubble formation, Figure 8). After 48 h, nuclear irregularities were no longer seen in both VERO and NIH/3T3 cells exposed to U2000-1 and U2000-2. All the cells analyzed from this time presented a round shape and a well-defined and regular nuclear surface, without signs of nuclear fragmentation and not suggesting pro-apoptotic effects. Although the non-polymerized adhesive initially moderately affects cell viability, once the in situ polymerization occurs, this toxicity tends to disappear. As no direct relationship between the excess of isocyanate and adhesiveness was experimentally observed, the use of lower levels of this monomer will be preferable to ensure cell survival and growth.

The cell affinity to the U2000-2 prepolymer was investigated in 24, 48, and 72 h post-seeding NIH/3T3 fibroblasts deposited onto the material surfaces by FEG-SEM (Figure 9) and DAPI staining (Figure 10). In the first 24 h of culture, the fibroblast showed a rounded morphology ($d_i = 1.04 \pm 0.1$ μm) and some adherent contact points with the adhesive surface.[22] Favorable cell affinity and growth pattern toward the adhesive were observed for 48 and 72 h, either by SEM or fluorescence results, with extensive cell spreading and releasing of extracellular matrix (ECM).[22,48] This biological mechanism is linked to the chemical nature and surface properties of the PU substrate, which confirms the surface free energy results. The high superficial energy from the polar chemical groups on the PU-based adhesive surface favors fibroblast affinity and attachment.[49,50] Moreover, the PU surface supports cell spreading due to the presence of polar urethane groups, which are

Figure 8. VERO cells exposed to reactive U2000-2 for 24 h. Representative images of morphological signs of apoptosis ((a) magnification 20×, (b) magnification 40×) with disintegrated nuclei and the presence of cytoplasmic blebs (red arrow).

Figure 9. Fibroblasts NIH/3T3 morphology in U2000-2 at (a) 24, (b) 48, and (c) 72 h (FEG-SEM magnification 20.0k×)
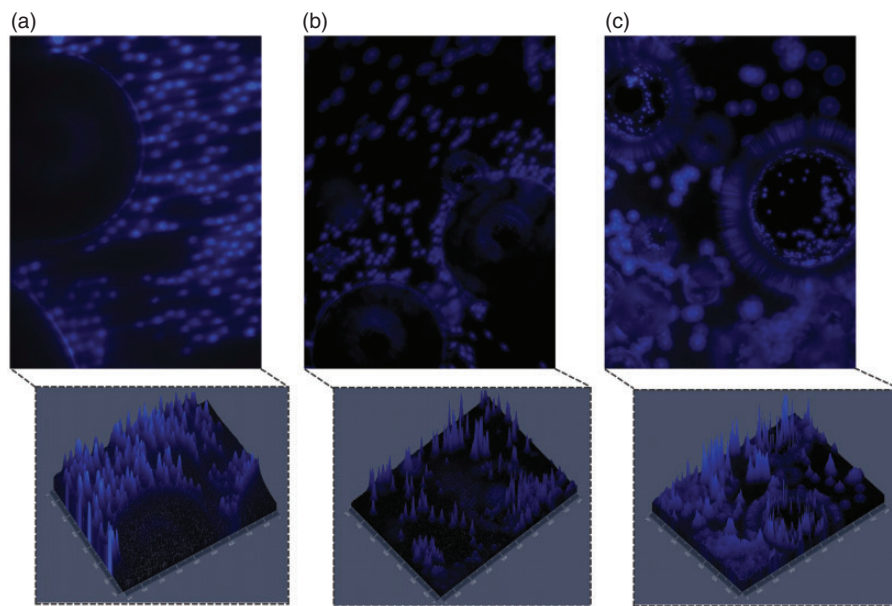
Figure 10. Fibroblasts NIH/3T3 adhesion in U2000-2 at (a) 24 h, (b) 48 h, and (c) 72 h. Cell nuclei were stained with DAPI (blue) (magnification 20×).

distributed throughout the soft domains. The high elasticity of the PU microstructure can tolerate the tension forces imposed by the cells.[51]

Conclusions

A PU-based tissue adhesive for AF repair has been evaluated through physicochemical, mechanical, thermal, rheological, and biological assays. The outstanding features of U2000-2 prepolymer result from its dynamic compress behavior, excellent adhesiveness to gelatin, minimum swelling, and injectability. This adhesive bounded gelatin covalently without the use of a catalyst or initiator. The U2000-2 formulation presented a shelf life stability of 18 days and required 10 h of preparation time at 60°C before use. This material also showed a moderate cytotoxic effect for NIH/3T3 fibroblasts in the first 24 h, which disappeared after polymerization. Favorable cell adhesion and proliferation toward the adhesive were observed after 48 h of culture. Although current findings provide preliminary evidence of the U2000-2 suitability, we agree that further research is needed, mainly to better understand the mechanical behavior of this adhesive. PU-based materials were relatively rigid, suggesting tunability of the compressive modulus. The results motivate future investigation to assess the performance with in situ biomechanical testing and in vivo biocompatibilty analyses, thus, evaluating these materials in more clinically relevant conditions. The sterility of these materials is being investigated. Such an interdisciplinary approach, requiring contributions from the biological and engineering areas, will continue to be necessary for the development of new clinical methods for AF repair.

Author's note

Lucas Dall Agnol, Sidnei Moura e Silva and Asdrubal Falavigna are affiliated to Health Sciences Graduate Program, University of Caxias do Sul (UCS), Caxias do Sul, RS, Brazil. Fernanda Trindade Gonzalez Dias and Otávio Bianchi are affiliated to Materials Science Graduate Program (PGMAT), University of Caxias do Sul (UCS), Caxias do Sul, RS, Brazil. Natália Fontana Nicoletti is affiliated to Cell Therapy Laboratory (LATEC), University of Caxias do Sul (UCS), Caxias do Sul, Brazil. Daniel Marinowic is affiliated to Brain Institute of Rio Grande do Sul (BraIns), Pontifical Catholic University of Rio Grande do Sul, Porto Alegre, RS, Brazil. Angel Marcos-Fernandez is affiliated to Instituto de Ciencia y Tecnología de Polímeros (CSIC), Madrid, Spain.

ORCID iD

Lucas Dall Agnol https://orcid.org/0000-0001-6024-9375

Supplemental material

Supplemental material for this article is available online.

References

1. Carragee EJ, Don AS, Hurwitz EL, et al. 2009 ISSLS prize winner: does discography cause accelerated progression of degeneration changes in the lumbar disc: a ten-year matched cohort study. *Spine* 2009; 34: 2338–2345.

2. Carragee EJ, Han MY, Suen PW, et al. Clinical outcomes after lumbar discectomy for sciatica: the effects of fragment type and anular competence. *J Bone Joint Surg* 2003; 85: 102–108.

3. Bartlett RD, Choi D and Phillips JB. Biomechanical properties of the spinal cord: implications for tissue engineering and clinical translation. *Regen Med* 2016; 11: 659–673.

4. Huang YC, Urban JP and Luk KD. Intervertebral disc regeneration: do nutrients lead the way? *Nat Rev Rheumatol* 2014; 10: 561–566.

5. Guterl CC, Torre OM, Purmessur D, et al. Characterization of mechanics and cytocompatibility of fibrin-genipin annulus fibrosus sealant with the addition of cell adhesion molecules. *Tissue Eng Part A* 2014; 20: 2536–2545.

6. Bailey A, Araghi A, Blumenthal S, et al. Prospective, multicenter, randomized, controlled study of anular repair in lumbar discectomy: two-year follow-up. *Spine* 2013; 38: 1161–1169.

7. Bron JL, van der Veen AJ, Helder MN, et al. Biomechanical and *in vivo* evaluation of experimental closure devices of the annulus fibrosus designed for a goat nucleus replacement model. *Eur Spine J* 2010; 19: 1347–1355.

8. Guterl CC, See EY, Blanquer SB, et al. Challenges and strategies in the repair of ruptured annulus fibrosus. *Eur Cell Mater* 2013; 25: 1–21.

9. Long RG, Torre OM, Hom WW, et al. Design requirements for annulus fibrosus repair: review of forces, displacements, and material properties of the intervertebral disk and a summary of candidate hydrogels for repair. *J Biomech Eng* 2016; 138: 021007.

10. Agnol LD, Dias FTG, Nicoletti NF, et al. Polyurethane as a strategy for annulus fibrosus repair and regeneration: a systematic review. *Regen Med* 2018; 13: 611–626. (05):

11. Bhagat V and Becker ML. Degradable adhesives for surgery and tissue engineering. *Biomacromolecules* 2017; 18: 3009–3039.

12. Agger RT. Survey of polyurethane adhesives. *Int J Adhes Adhes* 1984; 4: 151–152.

13. Wang T, Nie J and Yang D. Dextran and gelatin based photocrosslinkable tissue adhesive. *Carbohydr Polym* 2012; 90: 1428–1436.

14. Wang X, Partlow B, Liu J, et al. Injectable silk-polyethylene glycol hydrogels. *Acta Biomater* 2015; 12: 51–61.

15. Matsuda T, Nakajima N, Itoh T, et al. Development of a compliant surgical adhesive derived from novel fluorinated hexamethylene diisocyanate. *Asaio J* 1989; 35: 381–383.

16. Bochynska AI, Sharifi S, van Tienen TG, et al. Development of tissue adhesives based on amphiphilic isocyanate-terminated trimethylene carbonate block copolymers. *Macromol Symp* 2013; 334: 40–48.

17. Ozawa T. A new method of analyzing thermogravimetric data. *BCSJ* 1965; 38: 1881–1886.

18. Friedman HL. Kinetics of thermal degradation of char-forming plastics from thermogravimetry. Application to a phenolic plastic. *J Polym Sci, C Polym Symp* 1964; 6: 183–195.

19. Kissinger HE. Reaction kinetics in differential thermal analysis. *Anal Chem* 1957; 29: 1702–1706.

20. Ferreira P, Silva AF, Pinto MI, et al. Development of a biodegradable bioadhesive containing urethane groups. *J Mater Sci: Mater Med* 2008; 19: 111–120.

21. Owens DK and Wendt RC. Estimation of the surface free energy of polymers. *J Appl Polym Sci* 1969; 13: 1741–1747.

22. Dias FTG, Ingracio AR, Nicoletti NF, et al. Soybean-modified polyamide-6 mats as a long-term cutaneous wound covering. *Mater Sci Eng C Mater Biol Appl* 2019; 99: 957–968.

23. Ferreira P, Pereira R, Coelho J, et al. Modification of the biopolymer castor oil with free isocyanate groups to be applied as bioadhesive. *Int J Biol Macromol* 2007; 40: 144–152.

24. Oh SY, Kang MS, Knowles JC, et al. Synthesis of bio-based thermoplastic polyurethane elastomers containing isosorbide and polycarbonate diol and their biocompatible properties. *J Biomater Appl* 2015; 30: 327–337.

25. Špírková M, Poręba R, Pavličević J, et al. Aliphatic polycarbonate-based polyurethane elastomers and nanocomposites. I. The influence of hard-segment content and macrodiol-constitution on bottom-up self-assembly. *J Appl Polym Sci* 2012; 126: 1016–1030.

26. Iatridis JC, Setton LA, Weidenbaum M, et al. The viscoelastic behavior of the non-degenerate human lumbar nucleus pulposus in shear. *J Biomech* 1997; 30: 1005–1013.

27. Silva-Correia J, Oliveira JM, Caridade S, et al. Gellan gum-based hydrogels for intervertebral disc tissue-engineering applications. *J Tissue Eng Regen Med* 2011; 5: 97–107.

28. Best BA, Guilak F, Setton LA, et al. Compressive mechanical properties of the human anulus fibrosus and

their relationship to biochemical composition. *Spine* 1994; 19(2): 212–221.

29. Ferreira P, Coelho J, Pereira R, et al. Synthesis and characterization of a poly(ethylene glycol) prepolymer to be applied as a bioadhesive. *J Appl Polym Sci* 2007; 105: 593–601.

30. Green TP, Adams MA and Dolan P. Tensile properties of the annulus fibrosus. *Eur Spine J* 1993; 2: 209–214.

31. Wilke HJ, Neef P, Caimi M, et al. New *in vivo* measurements of pressures in the intervertebral disc in daily life. *Spine* 1999; 24: 755–762.

32. Damink LO, Dijkstra P, Van Luyn M, et al. Crosslinking of dermal sheep collagen using hexamethylene diisocyanate. *J Mater Sci: Mater Med* 1995; 6: 429–434.

33. Kuijpers AJ, Engbers GH, Krijgsveld J, et al. Crosslinking and characterisation of gelatin matrices for biomedical applications. *J Biomater Sci Polym Ed* 2000; 11: 225–243.

34. Spencer P, Byerley T, Eick J, et al. Chemical characterization of the dentin/adhesive interface by fourier transform infrared photoacoustic spectroscopy. *Dent Mater* 1992; 8: 10–15.

35. Chattopadhyay DK and Raju K. Structural engineering of polyurethane coatings for high performance applications. *Prog Polym Sci* 2007; 32: 352–418.

36. Mendoza-Novelo B, Alvarado-Castro DI, Mata-Mata JL, et al. Stability and mechanical evaluation of bovine pericardium cross-linked with polyurethane prepolymer in aqueous medium. *Mater Sci Eng C Mater Biol Appl* 2013; 33: 2392–2398.

37. Li Y and Huang Y. Preparation of collagen–polyurethane composite film and its subcutaneous implantation in rats: the improvement of tissue compatibility. *J Appl Polym Sci* 2006; 99: 1832–1841.

38. Chan-Chan LH, González-García G, Vargas-Coronado RF, et al. Characterization of model compounds and poly(amide-urea) urethanes based on amino acids by FTIR, NMR and other analytical techniques. *Eur Polym J* 2017; 92: 27–39.

39. Sarkar S, Chourasia A, Maji S, et al. Synthesis and characterization of gelatin based polyester urethane scaffold. *Bull Mater Sci* 2006; 29: 475–484.

40. Mendoza-Novelo B, Mata-Mata JL, Vega-González A, et al. Synthesis and characterization of protected oligourethanes as crosslinkers of collagen-based scaffolds. *J Mater Chem B* 2014; 2: 2874–2882.

41. Kratochvil A and Hrncir E. Correlation between the blood surface tension and the activity of some enzymes. *Physiol Res* 2001; 50: 433–437.

42. Daniel-da-Silva AL, Bordado JCM, Martín-Martinez JM, et al. Moisture curing kinetics of isocyanate ended urethane quasiprepolymers monitored by IR spectroscopy and DSC. *J Appl Polym Sci* 2008; 107: 700–709.

43. d'Arlas BF, Rueda L, Stefani PD, et al. Kinetic and thermodynamic studies of the formation of a polyurethane based on 1,6-hexamethylene diisocyanate and poly (carbonate-co-ester)diol. *Thermochim Acta* 2007; 459: 94–103.

44. Erceg M, Krešić I, Vrandečić NS, et al. Different approaches to the kinetic analysis of thermal degradation of poly (ethylene oxide). *J Therm Anal Calorim* 2018; 131: 325–334.

45. Chen Q, Liang S and Thouas GA. Elastomeric biomaterials for tissue engineering. *Prog Polym Sci* 2013; 38: 584–671.

46. Guo R, Ward CL, Davidson JM, et al. A transient cell-shielding method for viable MSC delivery within hydrophobic scaffolds polymerized *in situ*. *Biomaterials* 2015; 54: 21–33.

47. Mohsen NM, Craig RG and Hanks C. Cytotoxicity of urethane dimethacrylate composites before and after aging and leaching. *J Biomed Mater Res* 1998; 39: 252–260.

48. Asefnejad A, Khorasani MT, Behnamghader A, et al. Manufacturing of biodegradable polyurethane scaffolds based on polycaprolactone using a phase separation method: physical properties and *in vitro* assay. *Int J Nanomedicine* 2011; 6: 2375–2384.

49. Yang L, Kandel RA, Chang G, et al. Polar surface chemistry of nanofibrous polyurethane scaffold affects annulus fibrosus cell attachment and early matrix accumulation. *J Biomed Mater Res A* 2009; 91: 1089–1099.

50. Sheikh N, Mirzadeh H, Katbab A, et al. Isocyanate-terminated urethane prepolymer as bioadhesive material: evaluation of bioadhesion and biocompatibility, *in vitro* and *in vivo* assays. *J Biomater Sci Polym Ed* 2001; 12: 707–719.

51. Sheikh N. The effect of radiosterilization on cytotoxicity of polyurethane film. *Nucl Instrum Methods Phys Res B* 2003; 208: 215–219.